ACS APPLIED MATERIALS & INTERFACES

www.acsami.org

Research Article

Graphene Interlocking Carbon Nanotubes for High-Strength and High-Conductivity Fibers

Lijun Li, Tongzhao Sun, Shichao Lu, Zhuo Chen, Shichen Xu, Muqiang Jian,* and Jin Zhang*

Cite This: *ACS Appl. Mater. Interfaces* 2023, 15, 5701−5708

Read Online

ACCESS | Metrics & More | Article Recommendations | Supporting Information

ABSTRACT: Carbon nanotubes (CNTs) are promising building blocks for the fabrication of novel fibers with structural and functional properties. However, the mechanical and electrical performances of carbon nanotube fibers (CNTFs) are far lower than the intrinsic properties of individual CNTs. Exploring methods for the controllable assembly and continuous preparation of high-performance CNTFs is still challenging. Herein, a graphene/chlorosulfonic acid-assisted wet-stretching method is developed to produce highly densified and well-aligned graphene/carbon nanotube fibers (G/CNTFs) with excellent mechanical and electrical performances. Graphene with small size and high quality can bridge the adjacent CNTs to avoid the interfacial slippage under deformation, which facilitates the formation of a robust architecture with abundant conductive pathways. Their ordered structure and enhanced interfacial interactions endow the fibers with both high strength (4.7 GPa) and high electrical conductivity (more than 2×10^6 S/m). G/CNTF-based lightweight wires show good flexibility and knittability, and the high-performance fiber heaters exhibit ultrafast electrothermal response over 1000 °C/s and a low operation voltage of 3 V. This method paves the way for optimizing the microstructures and producing high-strength and high-conductivity CNTFs, which are promising candidates for the high-value fiber-based applications.

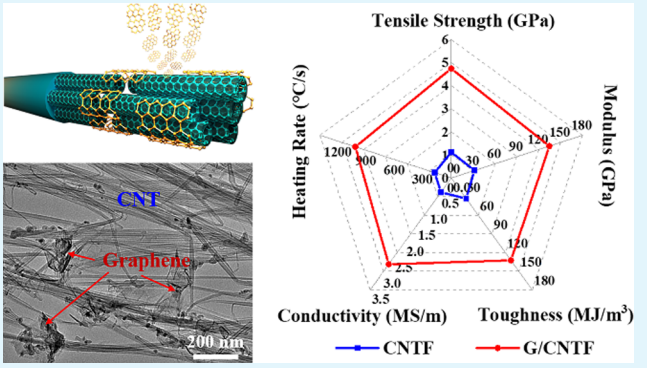

KEYWORDS: *carbon nanotube fibers, graphene, high strength, high conductivity, heaters*

INTRODUCTION

Carbon nanotubes (CNTs), featuring an excellent combination of low density, superior flexibility, ultrahigh strength and modulus, and good thermal and electrical conductivities, have been well known as the ideal building block for the next-generation high-performance fibers.[1−5] Owing to these outstanding features, carbon nanotube fibers (CNTFs) could achieve plenty of engineering applications in bulletproof vests, lightweight wires, artificial muscles, energy systems, flexible electronics, etc.[6−13] Various techniques have been developed to produce CNTFs, such as spinning from the CNT liquid crystal dope,[14,15] spinning from the vertically aligned CNT arrays,[16] and direct spinning from the CNT aerogels.[17−21] Generally, the direct spinning process offers a feasible way to realize the continuous and scalable production of CNTFs. However, so far, the properties of CNTFs, particularly their strength and electrical conductivity, are still not a circumstance to individual CNTs,[1,3,9] strongly hindering their niche applications. The great challenges are mainly lying in the poor packing density, weak interfacial shear strength, and low degree of alignment.[22] Therefore, it is of vital importance to optimize the assembly structure and intertube interactions between individual CNTs to obtain high-performance CNTFs.

There have been numerous post-treatment approaches for the reconstruction of architectured CNT ensembles and the enhancement of their interactions, which open up avenues for effectively extending the superior properties of nanoscale CNTs to macroscopic CNTFs. The solution densification,[23−27] mechanical treatment,[28,29] and thermal annealing process[30,31] have been used to improve the packing density and orientation of CNTFs. Notably, chlorosulfonic acid (CSA) enables the side-wall protonation of CNTs and induces the remarkable volume expansion of the as-spun fibers, which offers a unique opportunity to reassemble the internal microstructures. Lee et al.[27] immersed the obtained CNTFs into CSA and introduced a feasible stretching process to produce a significant increase in specific strength (4.08 N/tex), modulus, and electrical conductivity, showing an extraordinary strengthening effect. In another strategy, the infiltration of

Received: November 30, 2022
Accepted: January 11, 2023
Published: January 20, 2023

polymers (such as polyvinyl alcohol,[32] epoxy,[33] bismaleimide,[34] and silk fibroin[35]), cross-linking agents,[36] or nanocarbon materials (such as graphene,[37] graphene oxide (GO),[38−40] and amorphous carbon[41−45]) has been developed to fabricate the highly densified and aligned CNTFs, as well as induce the stronger interaction between neighboring CNTs through formation of $\pi-\pi$ interactions, hydrogen bonding or even covalent bonds. However, the conductivity of CNTFs inevitably deteriorates owing to the introduction of polymers or GO. Besides, the foreign components, especially the graphene-based materials, predominantly exist on the surface of fibers rather than integrating into the inside and have a small room to refine the internal structures and exert relatively little effect on improving the performance of CNTFs. Therefore, it is still a considerable challenge to simultaneously improve the compactness, orientation, and intertube interaction to produce high-strength and highly conductive CNTFs.

In this work, we develop a graphene/CSA-assisted wet-stretching (GAWS) method that involves introducing graphene, stretching, and densification processes to fabricate the graphene/carbon nanotube fiber (G/CNTF) with high strength and high conductivity. First, small-sized and high-quality graphene dispersed in CSA is successfully integrated into CNTFs as the fibers swell by the protonation of CSA. Then, appropriate stretching is introduced to induce the high alignment of CNTs, and subsequently, fibers are immersed into a coagulation bath to improve the packing density. Consequently, highly dense and well-ordered fibers with fascinating properties are obtained. It is proved that graphene can bridge the adjacent CNTs and thus avoid intertube slippage under tension, endowing the fibers with a remarkable tensile strength (4.7 GPa). In addition, incorporation of graphene has the capability of forming continuous conductive pathways and resulting in the high conductivity (2.7×10^6 S/m), which is five times higher than that of the pristine counterparts. This G/CNTF can be used as the fiber heater with good flexibility, desirable knittability, and ultrafast thermal response (a heating rate of 1022 °C/s at a voltage of 3 V), which could be further woven into textiles.

RESULTS AND DISCUSSION

Fabrication of G/CNTFs. Figure 1a schematically illustrates the continuous fabrication of G/CNTFs through a GAWS strategy involving acid-assisted expansion, graphene introduction, stretching, and densification, toward the closely packed and highly aligned fibers with desirable properties. CNTFs produced by the direct spinning process are subjected to poor orientation, high entanglement, and low densification (stage I). When the as-spun fiber was immersed in CSA solution, the fiber swelled visibly and delivered about a 10-fold increase in diameter (Figure S1, Supporting Information) as CSA protonated the nanotube walls and induced the repulsive forces between them.[27,46−48] The expanded CNTFs offer a unique opportunity for the small-sized graphene penetration to construct a hetero-dimensional hybrid fiber. The small-sized graphene was prepared by a microwave-induced "snowing" process,[49,50] exhibiting an average size of about 350 nm (Figures 1b and S2b−d, Supporting Information). The obtained graphene exhibits high quality, yielding a low intensity ratio of I_D/I_G (about 0.26) (Figure S2a, Supporting Information). Additionally, X-ray photoelectron spectroscopy (XPS) reveals that graphene has a high element ratio of C/O (about 46.2) and no impurity elements are introduced (Figure S2e, Supporting Information), indicating the high purity of graphene. Particularly, a strong sp^2 carbon peak (284.8 eV) can be found in the C1s spectrum (Figure S2f, Supporting Information). Similarly, CSA enabled the protonation of the high-quality graphene and facilitated to form a homogeneous dispersion,[51] which was highly stable even after 3 months (Figure S3, Supporting Information). When a CNTF was immersed into the graphene/CSA solution, small-sized graphene penetrated into the expended fiber readily and acted as the interlocking materials to bridge and strengthen the adjacent CNTs (state II, Figure 1c). Note that an appropriate stretching was introduced to improve the alignment of CNTs and reassemble the microstructures of CNTF. After densification in coagulating bath and drying process, G/CNTFs with high strength and conductivity were collected (stage III). Compared with the pristine CNTFs, G/CNTFs show the overwhelming superiority in tensile strength, Young's modulus, toughness, electrical conductivity, and heating rate (Figure 1d), revealing that the GAWS method is a feasible and effective strategy to produce the G/CNTFs with superior mechanical and electrical properties.

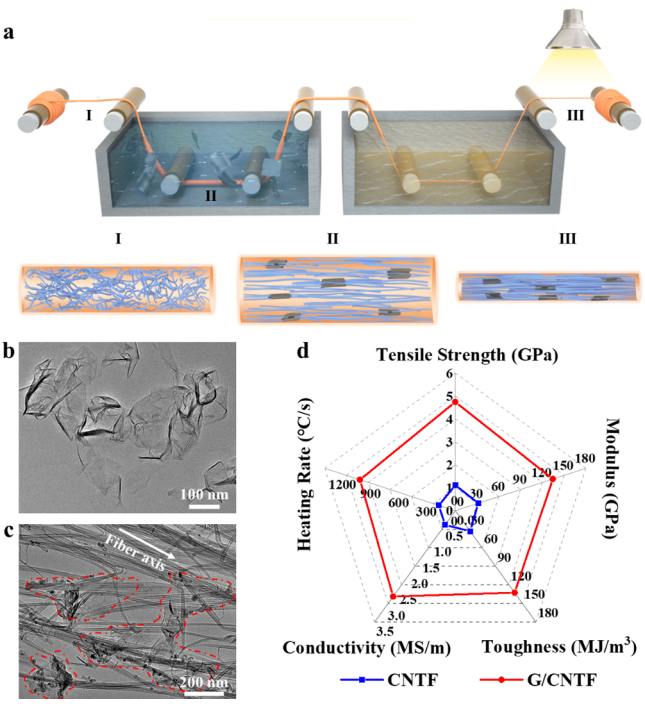

Figure 1. Fabrication of G/CNTFs with excellent properties. (a) Schematic illustration of the continuous production of highly dense and well-aligned G/CNTFs through the GAWS method, which is the integration of acid-assisted expansion together with the graphene incorporation, axial stretching, and consequent densification process. (b,c) Transmission electron microscopy (TEM) images of small-sized graphene (b) and the assembly structure of G/CNTFs (c). (d) Radial plot comparing the tensile strength, modulus, toughness, electrical conductivity, and heating rate for a pristine CNTF and a G/CNTF.

The microstructures of CNTF and G/CNTF are compared in Figure 2. Generally, the aerogel-spun fibers with a diameter of 31.5 μm show plenty of voids and high entanglements (Figures 2a and S4a, Supporting Information). Besides, consistent with the surface of microstructures, the inside of as-spun CNTFs suffer from a number of voids and poor orientation, which can be observed from the cross-sections of CNTFs cut by a focused ion beam (FIB) (Figures 2b and S4b,

https://doi.org/10.1021/acsami.2c21518
ACS Appl. Mater. Interfaces 2023, 15, 5701−5708

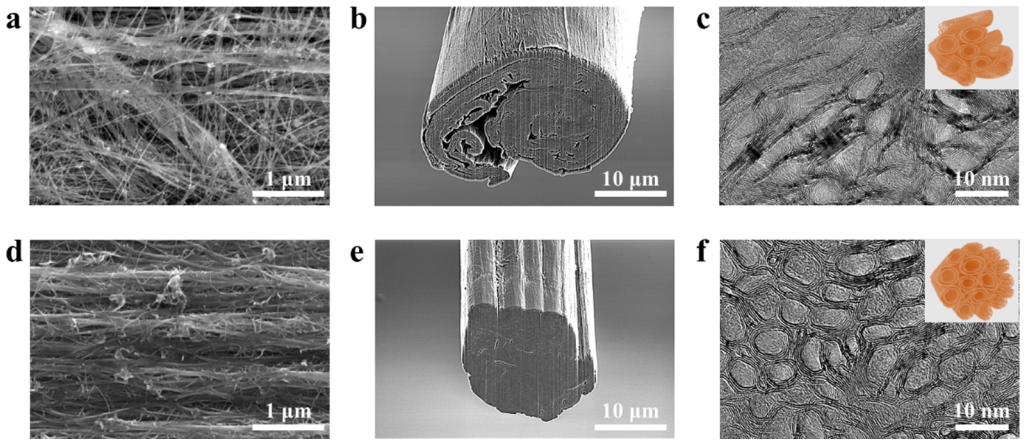

Figure 2. Comparison of the morphology of CNTFs and G/CNTFs. (a) Scanning electron microscopy (SEM) image showing the surface of microstructures. (b,c) SEM image (b) and TEM image (c) of the cross-sections of CNTFs, which were cut by a focused ion beam (FIB). (d) SEM image of the surface of G/CNTFs. (e,f) Cross-sectional SEM image (e) and TEM image (f) of G/CNTFs. Insets in (c) and (f) are the corresponding cross-sectional diagram of CNTFs and G/CNTFs, respectively.

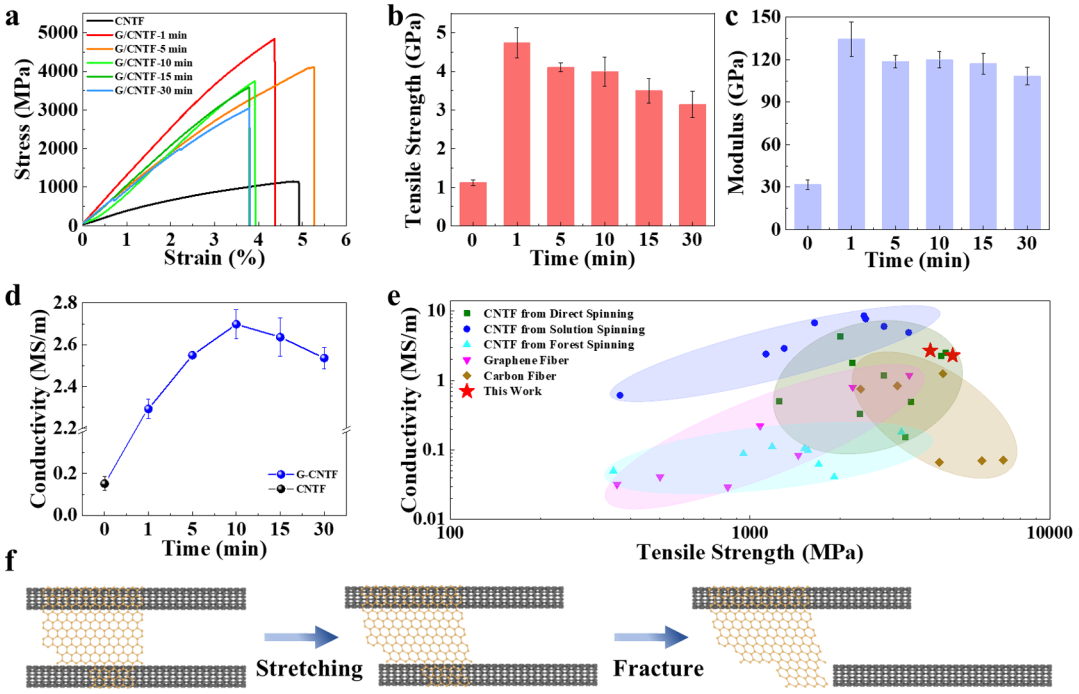

Figure 3. Mechanical and electrical properties of different fibers. (a) Stress versus strain curves of CNTFs and G/CNTFs. (b–d) Comparison of tensile strength (b), Young's modulus (c), and electrical conductivities (d) of CNTFs and G/CNTFs. (e) Comparison of tensile strength and electrical conductivity of G/CNTFs and the previously reported CNTFs, graphene fibers, and carbon fibers. (f) Proposed enhancement mechanism of graphene interlocking CNTs during a stretching process.

Supporting Information). Cross-sectional TEM image shows CNT bundles are highly entangled and only a few of CNTs orient the axis of fibers (Figure 2c). When the fibers are immersed into CSA bath with a certain stretching and subsequently a densified process, the diameter of obtained CNTFs (CSA/CNTFs) reduces remarkably (Figure S5, Supporting Information). The stretching ratio plays a vital role in the microstructures and performance of CNTFs. Notably, as the stretching ratios increase, the tensile strength of fibers will improve dramatically, and the fibers exhibit the highest tensile strength at the stretching ratio of 18% (Figure S6, Supporting Information). As can be seen in Figure S7, the obtained CSA/CNTFs, produced by the CSA-assisted wet-stretching and densification method, show a significant increase in packing density and alignment. However, there are some pores inside the fibers, which has an adverse effect on fabricating high-performance fibers.

When the fibers are pulled out from the graphene bath and subsequently densified, the voids in the G/CNTFs are reduced remarkably compared with the pristine fibers and CSA/CNTFs (Figures 2d–e and S8, Supporting Information). In addition, it is observed that CNTs are closely packed and most of them align in the fiber, indicating that the GAWS process is highly effective to improve the alignment of CNTs (Figure 2f). It can be inferred that the GAWS process accounts for the microstructure refinement, and graphene interlocks the neighboring CNTs to form a highly compact and well-aligned structures. Furthermore, the alignment of different fibers was

https://doi.org/10.1021/acsami.2c21518
ACS Appl. Mater. Interfaces 2023, 15, 5701–5708

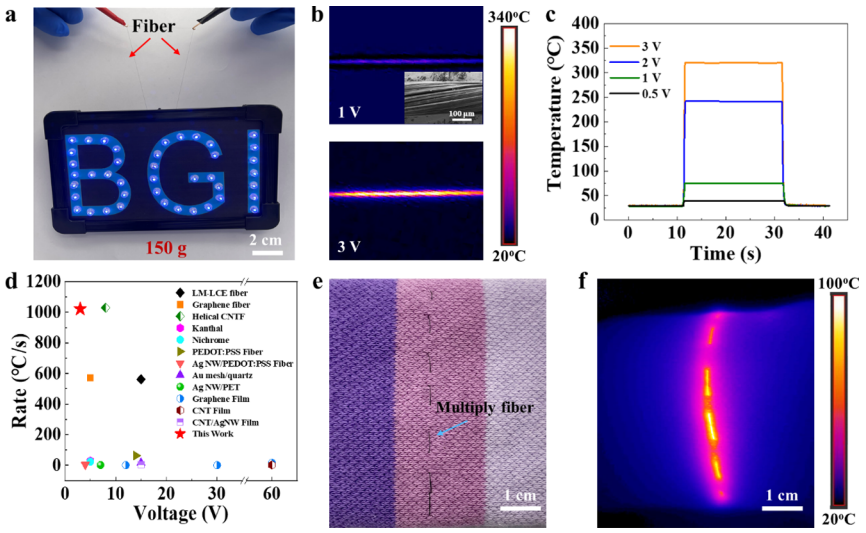

Figure 4. G/CNTFs for the lightweight and high load-bearing wires and high-performance heating fibers. (a) Photograph of a single G/CNTF lifting a 150 g weight and simultaneously serving as a lightweight wire to light up LEDs at a low voltage of 3 V, demonstrating the high mechanical strength and high conductivity. (b) Infrared images of a multiply fiber twisted from 18 fibers at 1 and 3 V. The inset is the SEM image of a multiply fiber. (c) Temperature profiles of fibers at different voltages. (d) Comparison of heating rates and applied voltages of the G/CNTF-based heater with different reported heating materials (more information in Table S2, Supporting Information).[57−62,66] LM-LCE, liquid metal-liquid crystal elastomer; PEDOT/PSS, poly(3,4-ethylenedioxythiophene)/poly(styrenesulfonate); Ag NW, Ag nanowire; PET, poly(ethylene terephthalate). (e) Photograph of a multiply fiber embroidered a fabric. (f) Infrared image of the textile at a voltage of 4 V.

assessed by the fast Fourier transform (FFT) of the SEM images and polarized Raman spectroscopy.[52,53] Figure S9 compares the FFT spectra and intensity distribution diagram of the three fibers. Obviously, the fibers produced by the acid-assisted expansion and densification method (CSA/CNTFs and G/CNTFs) exhibit more concentrated energy distributions and narrower distributions, revealing the higher orientation than the pristine counterparts. Additionally, ratios of $I_{G\parallel}$and $I_{G\perp}$ (intensities of the G peak of the Raman spectrum for the fibers axis aligned parallelly and perpendicularly to the polarization direction of laser beam, respectively) of CSA/CNTFs and G/CNTFs increase viably in comparison with the pristine ones (Figure S10). Therefore, the GAWS method offers a feasible strategy for the fabrication of highly dense and well-aligned fibers.

Mechanical and Electrical Properties of G/CNTFs. The orderly assembly structures of G/CNTFs endorse the substantial improvement in tensile strength. As the fibers are immersed in graphene dispersion with a concentration of 0.02 wt % for 1 min, G/CNTFs achieve the highest tensile strength of 4.7 GPa and Young's modulus of 134 GPa, which are 4.27 and 4.32 times that for the pristine CNTFs (1.1 and 31 GPa) (Figure 3a−c), respectively, and are much higher than those of CSA/CNTFs (Figure S11a−c, Supporting Information). Young's modulus of G/CNTFs is comparable to that of commercially available Kevlar and ultrahigh molecular weight polyethylene fibers and outperforms that for the carbon fiber fabric composites.[54] Moreover, the tensile strength and modulus decrease as the immersion times increase from 1 to 30 min with a stretching ratio of 18%, which can be ascribed to the graphene agglomeration influencing the uniformity of the internal structure with the increase of treatment times (Figure S12, Supporting Information). In addition, the effects of different graphene concentrations and sizes on the mechanical properties of fibers were also investigated. With the increase of concentrations (0.05 and 0.08 wt %), the tensile strength of G/CNTFs decreases gradually (Figure S13, Supporting Information). Indeed, graphene is inclined to agglomerate in CNTFs as the concentrations increase, which is analogous to the fibers treated by a low graphene content for a longer time. Additionally, the tensile strength of G/CNTFs produced by the smaller-sized graphene decrease gradually because of their agglomerates inside the fibers (Figure S14, Supporting Information).

In addition to their excellent mechanical properties, G/CNTFs offer a high electrical conductivity of 2.7 MS/m, which is 6.0 times that of the as-spun fibers (0.45 MS/m) and is superior to that of CSA/CNTFs (Figures 3d and S11d, Supporting Information). Figure 3e compares the tensile strength and electrical conductivity of the typical G/CNTFs with those of various carbon-based fibers, including CNTFs produced by different spinning methods, graphene fibers, and carbon fibers (detailed information showing in Table S1, Supporting Information). Our elaborated G/CNTFs have high strength and excellent conductivity, exceeding those of most state-of-the-art carbon-based fibers.

The fracture morphologies of different fibers were investigated to explore the strengthening effect. When the as-spun CNTFs are subjected to the axis tension, CNTs can slip between each other and single nanotube or small bundles are pulled out (Figure S15a,b, Supporting Information). After the acid-assisted expansion and densification processes, the fracture morphology of CSA/CNTFs shows that the CNTs assemble into large bundles (Figure S15c,d, Supporting Information). As shown in Figure 3f, when a tensile load is exerted on the G/CNTFs, graphene interlocking CNTs can prevent the bundles from slipping between each other (Figures 3f and S15e,f, Supporting Information) and enable the fibers to withstand greater stress, leading to the effective redistribution of local stress.[55] It can be clearly seen that the introduction of graphene is feasible to improve the load transfer efficiency, endowing the fibers with high mechanical properties. In addition, embedding graphene in the carbon nanotube matrix has the capability of bridging the adjacent CNTs and

https://doi.org/10.1021/acsami.2c21518
ACS Appl. Mater. Interfaces 2023, 15, 5701−5708

facilitating the formation of interconnected conductive pathways, as well as decreasing the hopping distance of charge carriers,[56] resulting in a significant increase in the electrical conductivity of G/CNTFs.

Applications in High-Performance Wires and Heaters. To demonstrate the outstanding properties of treated fibers, G/CNTFs were designed as lightweight wires and fiber heaters. As shown in Figure 4a, a single fiber can lift a 150 g weight and simultaneously act as the lightweight wire to turn on the light-emitting diodes (LEDs) at a low voltage of 3 V, indicating the high strength and high electrical conductivity of G/CNTFs. Furthermore, benefiting from their excellent flexibility and conductivity, G/CNTFs are suitable for the fabrication of high-performance heaters. A multiply fiber with a diameter of about 170 μm twisted from 18 fibers was processed into the fiber heater with copper foils utilized as electrodes. The two electrodes were connected to a direct current power supply. With applying a voltage on the G/CNTF-based heater (length of 2 cm), temperature distribution of the heater can be monitored by an infrared thermal camera in real time (Figures 4b and S16a, Supporting Information), and the saturated temperature reached immediately (Figure 4c). As the applied voltages are 0.5, 1, 2, and 3 V, the saturated temperatures of G/CNTF-based heaters increase from 38, 73, 242, to 321 °C, revealing the extremely high electrothermal efficiency. Significantly, along with the increase of diameters, the saturated temperature will be improved because of the enhanced current-carrying capacity.[57] As a comparison, the achieved temperatures of CNTF-based heaters are only 24, 32, 59, and 79 °C with the corresponding voltages (Figure S16b,c, Supporting Information), which are much inferior to those of G/CNTF-based heaters. Importantly, the G/CNTF-based heater possesses a high electrothermal response, and the heating rate can reach 1022 °C/s at a low voltage of 3 V, which is better than most fiber-based heaters, such as commercial Kanthal and nichrome wires (heating rates of 29.1 and 23.7 °C/s, respectively, at a voltage of 5 V),[58] graphene fiber (a heating rate of 571 °C/s at a voltage of 5 V),[58] metal-based films or fibers,[59,60] and graphene or CNT films[61,62] (Figure 4d and see detailed information in Table S2, Supporting Information). Besides, the heating rate of the G/CNTF-based heater is comparable with that of the hierarchically helical CNTF (about 1030 °C/s).[57] Indeed, our heater exhibits lower operation voltage and higher achieved temperature, demonstrating the outstanding electrothermal performance of G/CNTF-based heaters. This ultrafast thermal response is generally ascribed to high electrical and thermal conductivity,[63] ultrasmall heat capacity per unit area, and a large radiation coefficient.[64,65] Additionally, the cooling rate is comparable with the heating rate, which is attributed to the large emissivity due to the high absorbance.[64]

Given the excellent heating capability of our fiber heater, a multiply G/CNTF has been embroidered on the fabric (Figure 4e). As shown in Figure 4f, when a voltage of 4 V is applied on the fabric, the temperature of the fiber heater reaches about 100 °C, and the temperature can be easily controlled by altering the voltages, length and number of fibers, and so on. Additionally, G/CNTF-based heaters have good flexibility, showing substantial promises for the applications in high-performance heating clothing.

CONCLUSIONS

In this work, we propose a feasible GAWS strategy to construct the interconnected network by interlocking adjacent CNTs using the small-sized and high-quality graphene, resulting in the production of high-strength and high-conductivity fibers. The GAWS process enables the microstructure refinement and facilitates the fabrication of highly densified and well-ordered CNTFs. More importantly, graphene can bridge and reinforce the adjacent CNTs to impede the interfacial slippage under tension, as well as form the continuous conductive pathways. The GAWS method endorses the great improvement in mechanical and electrical properties, endowing the G/CNTFs with high strength (4.7 GPa) and high electrical conductivity (2.7 MS/m). Due to the outstanding properties, the G/CNTFs are successfully used as lightweight wires and high-performance fiber heaters. The G/CNTF-based heater shows the ultrafast electrothermal response and low operation voltage (a heating rate of 1022 °C/s at a voltage of 3 V), which can be easily integrated into flexible textiles. The GAWS strategy opens up a simple and facile method to produce high-performance CNT-based fibers, which are promising applications in high-performance and multifunctional composites, lightweight wires, and wearable electronics.

EXPERIMENTAL SECTION

Preparation of CNTFs. CNTFs were prepared by the floating catalyst chemical vapor deposition method.[67,68] The acetone solution containing ferrocene (0.5 wt %) and thiophene (1.0 wt %) was injected into the vertical reactor tube with a diameter of 100 mm. A mixture of hydrogen and argon with a total gas flow of 5 L/min was the carrier gas. CNTs nucleated and grew in the high-temperature reaction zone (1300 °C) and further formed sock-like hollow aerogels, which were then pulled out from the reaction tube and subsequently assembled into continuous CNTFs after passing through the water. Consequently, CNTFs were collected by a roller with a winding speed ranging from 15 to 25 m/min. Finally, CNTFs were dried at 400 °C for 1 min.

Preparation of Graphene. The small-sized and high-quality graphene was produced by a microwave-induced "snowing" process without any catalyst or substrate.[49,50] Argon was used to expel residual air in a quartz tube and then generate the plasma at ambient pressure. Methane was introduced into the tube for the preparation of graphene in the gas phase, which was "snowing," and graphene powder could be obtained.

Preparation of CSA/CNTFs and G/CNTFs. The as-spun CNTFs were immersed into CSA solution for 1, 5, 10, 15, or 30 min with different stretching ratios ranging from 10% to 20%. Then, the fibers were introduced into the acetone bath for densification. Finally, the fibers were dried and collected on a winder, which were termed CSA/CNTFs. Similarly, the pristine CNTFs were brought into the uniform graphene/CSA bath (with a concentration of 0.02 wt %) for different times (1, 5, 10, 15, or 30 min). Meanwhile, the CNTFs were subjected to the axial stretching to improve the alignment. The subsequent treatments were consistent with the aforementioned CSA/CNTFs, and these fibers were denoted as G/CNTFs. Additionally, the different G/CNTFs were prepared by different graphene concentrations (0.05 and 0.08 wt %) or sizes (40 and 110 nm).

Characterization. The fiber diameters were recorded by SEM (FEI Quattro S, Thermo Fisher Scientific). The morphologies of graphene and fibers were investigated by SEM and TEM (F20, Thermo Fisher Scientific). For the cross-sectional observation, fibers were cut by a FIB system ((Helios, Thermo Fisher Scientific). Raman spectroscopy (Horiba HR800) with a 532 nm laser was used to explore the degree of defects of graphene and fibers, and polarized Raman spectroscopy was used to assess the orientation of fibers. XPS (AXIS Supra photoelectron spectrometer with Al Kα source, Kratos

https://doi.org/10.1021/acsami.2c21518
ACS Appl. Mater. Interfaces 2023, 15, 5701−5708

Analytical Ltd.) was applied to evaluate the quality and element content of small-sized graphene. Atomic force microscopy (AFM) (Dimension Icon, Bruker) was used to obtain the average size of graphene. Additionally, we performed the FFT transform of SEM images using the Image J software for the comparison of the orientation of different fibers. Mechanical properties of different fibers were performed by a universal testing machine (SHIMADZU, EZ-LX) with a load sensor of 5 N. The gauge length was 10 mm and the strain rate was 1 mm·min^{-1}. The electrical conductivities of fibers were tested by a digital source meter (Keithley 2450) by the two-point probe method. The fiber heaters were connected to a direct current power supply (ANS, JP1505D) under ambient conditions, and the temperatures were monitored by an infrared imager (FLIRA615).

■ ASSOCIATED CONTENT

Supporting Information

The Supporting Information is available free of charge at https://pubs.acs.org/doi/10.1021/acsami.2c21518.

Additional experimental details including optical images; SEM and TEM images of different fibers and graphene; AFM and XPS results of graphene; Raman spectra of different fibers; mechanical and electrical properties of CSA/CNTFs; performance of CNT-based heating fibers; and performance comparison (PDF)

■ AUTHOR INFORMATION

Corresponding Authors

Muqiang Jian − *Beijing Graphene Institute (BGI), Beijing 100095, P. R. China*; Email: jianmq@bgi-graphene.com

Jin Zhang − *Beijing Graphene Institute (BGI), Beijing 100095, P. R. China; Center for Nanochemistry, Beijing Science and Engineering Center for Nanocarbons, Beijing National Laboratory for Molecular Sciences, College of Chemistry and Molecular Engineering and School of Materials Science and Engineering, Peking University, Beijing 100871, P. R. China;* orcid.org/0000-0003-3731-8859; Email: jinzhang@pku.edu.cn

Authors

Lijun Li − *Beijing Graphene Institute (BGI), Beijing 100095, P. R. China*

Tongzhao Sun − *Beijing Graphene Institute (BGI), Beijing 100095, P. R. China; State Key Laboratory of High-Efficiency Coal Utilization and Green Chemical Engineering, College of Chemistry and Chemical Engineering, Ningxia University, Yinchuan 750021, P. R. China*

Shichao Lu − *Beijing Graphene Institute (BGI), Beijing 100095, P. R. China*

Zhuo Chen − *Beijing Graphene Institute (BGI), Beijing 100095, P. R. China; Center for Nanochemistry, Beijing Science and Engineering Center for Nanocarbons, Beijing National Laboratory for Molecular Sciences, College of Chemistry and Molecular Engineering, Peking University, Beijing 100871, P. R. China*

Shichen Xu − *Beijing Graphene Institute (BGI), Beijing 100095, P. R. China; Center for Nanochemistry, Beijing Science and Engineering Center for Nanocarbons, Beijing National Laboratory for Molecular Sciences, College of Chemistry and Molecular Engineering, Peking University, Beijing 100871, P. R. China*

Complete contact information is available at: https://pubs.acs.org/10.1021/acsami.2c21518

Author Contributions

The manuscript was written through contributions of all authors. J.Z. and M.J. conceived the idea and designed the project. L.L. carried out the preparation of samples and characterization. T.S., S.L., and Z.C. provided the analysis of the experimental results. L.L., S. X., M.J., and J.Z. prepared the manuscript. All authors have reviewed and contributed to the final version of the manuscript.

Notes

The authors declare no competing financial interest.

■ ACKNOWLEDGMENTS

The authors thank Y. Y. Zhang, Z. Z. Yong, and T. Zhou from the Suzhou Institute of Nano-Tech and Nano-Bionics, Chinese Academy of Sciences, for help in providing CNTF samples. This work was financially supported by Beijing Natural Science Foundation (No. 2222094), the Ministry of Science and Technology of China (2016YFA0200100 and 2018YFA0703502), the National Natural Science Foundation of China (Nos. T2188101, 52021006, 52202032, 51720105003, 21790052, and 21974004), the Strategic Priority Research Program of CAS (XDB36030100), and the Beijing National Laboratory for Molecular Sciences (BNLMS-CXTD-202001).

■ REFERENCES

(1) Bai, Y.; Yue, H.; Zhang, R.; Qian, W.; Zhang, Z.; Wei, F. Mechanical Behavior of Single and Bundled Defect-Free Carbon Nanotubes. *Acc. Mater. Res.* **2021**, *2*, 998−1009.

(2) Wu, K.; Zhang, Y.; Yong, Z.; Li, Q. Continuous Preparation and Performance Enhancement Techniques of Carbon Nanotube Fibers. *Acta Phys.-Chim. Sin.* **2022**, *38*, No. 2106034.

(3) Bulmer, J. S.; Kaniyoor, A.; Elliott, J. A. A Meta-Analysis of Conductive and Strong Carbon Nanotube Materials. *Adv. Mater.* **2021**, *33*, No. 2008432.

(4) Wu, S.; Li, H.; Futaba, D. N.; Chen, G.; Chen, C.; Zhou, K.; Zhang, Q.; Li, M.; Ye, Z.; Xu, M. Structural Design and Fabrication of Multifunctional Nanocarbon Materials for Extreme Environmental Applications. *Adv. Mater.* **2022**, *34*, No. 2201046.

(5) Mikhalchan, A.; Vilatela, J. J. A Perspective on High-Herformance CNT Fibres for Structural Composites. *Carbon* **2019**, *150*, 191−215.

(6) Kim, J. G.; Yu, H.; Jung, J. Y.; Kim, M. J.; Jeon, D. Y.; Jeong, H. S.; Kim, N. D. 3D Architecturing Strategy on the Utmost Carbon Nanotube Fiber for Ultra-High Performance Fiber-Shaped Supercapacitor. *Adv. Funct. Mater.* **2022**, *32*, No. 2113057.

(7) Jang, Y.; Kim, S. M.; Spinks, G. M.; Kim, S. J. Carbon Nanotube Yarn for Fiber-Shaped Electrical Sensors, Actuators, and Energy Storage for Smart Systems. *Adv. Mater.* **2020**, *32*, No. 1902670.

(8) Zhang, X.; Lu, W.; Zhou, G.; Li, Q. Understanding the Mechanical and Conductive Properties of Carbon Nanotube Fibers for Smart Electronics. *Adv. Mater.* **2019**, *32*, No. 1902028.

(9) Qian, L.; Xie, Y.; Zou, M.; Zhang, J. Building a Bridge for Carbon Nanotubes from Nanoscale Structure to Macroscopic Application. *J. Am. Chem. Soc.* **2021**, *143*, 18805−18819.

(10) Chu, H.; Hu, X.; Wang, Z.; Mu, J.; Li, N.; Zhou, X.; Fang, S.; Haines, C. S.; Park, J. W.; Qin, S.; Yuan, N.; Xu, J.; Tawfick, S.; Kim, H.; Conlin, P.; Cho, M.; Cho, K.; Oh, J.; Nielsen, S.; Alberto, K. A.; Razal, J. M.; Foroughi, J.; Spinks, G. M.; Kim, S. J.; Ding, J.; Leng, J.; Baughman, R. H. Unipolar Stroke, Electroosmotic Pump Carbon Nanotube Yarn Muscles. *Science* **2021**, *371*, 494−498.

(11) Son, W.; Chun, S.; Lee, J. M.; Jeon, G.; Sim, H. J.; Kim, H. W.; Cho, S. B.; Lee, D.; Park, J.; Jeon, J.; Suh, D.; Choi, C. Twist-Stabilized, Coiled Carbon Nanotube Yarns with Enhanced Capacitance. *ACS Nano* **2022**, *16*, 2661−2671.

(12) Huang, J.; Li, J.; Xu, X.; Hua, L.; Lu, Z. In Situ Loading of Polypyrrole onto Aramid Nanofiber and Carbon Nanotube Aerogel Fibers as Physiology and Motion Sensors. *ACS Nano* **2022**, *16*, 8161−8171.
(13) Taylor, L. W.; Williams, S. M.; Yan, J. S.; Dewey, O. S.; Vitale, F.; Pasquali, M. Washable, Sewable, All-Carbon Electrodes and Signal Wires for Electronic Clothing. *Nano Lett.* **2021**, *21*, 7093−7099.
(14) Kim, S. G.; Choi, G. M.; Jeong, H. D.; Lee, D.; Kim, S.; Ryu, K. H.; Lee, S.; Kim, J.; Hwang, J. Y.; Kim, N. D.; Kim, D. Y.; Lee, H. S.; Ku, B. C. Hierarchical Structure Control in Solution Spinning for Strong and Multifunctional Carbon Nanotube Fibers. *Carbon* **2022**, *196*, 59−69.
(15) Behabtu, N.; Young, C. C.; Tsentalovich, D. E.; Kleinerman, O.; Wang, X.; Ma, A. W.; Bengio, E. A.; ter Waarbeek, R. F.; de Jong, J. J.; Hoogerwerf, R. E.; Fairchild, S. B.; Ferguson, J. B.; Maruyama, B.; Kono, J.; Talmon, Y.; Cohen, Y.; Otto, M. J.; Pasquali, M. Strong, Light, Multifunctional Fibers of Carbon Nanotubes with Ultrahigh Conductivity. *Science* **2013**, *339*, 182−186.
(16) Zhang, M.; Atkinson, K. R.; Baughman, R. H. Multifunctional Carbon Nanotube Yarns by Downsizing an Ancient Technology. *Science* **2004**, *306*, 1358−1361.
(17) Zhang, X.; Li, Q.; Holesinger, T. G.; Arendt, P. N.; Huang, J.; Kirven, P. D.; Clapp, T. G.; DePaula, R. F.; Liao, X.; Zhao, Y.; Zheng, L.; Peterson, D. E.; Zhu, Y. Ultrastrong, Stiff, and Lightweight Carbon-Nanotube Fibers. *Adv. Mater.* **2007**, *19*, 4198−4201.
(18) Smail, F.; Boies, A.; Windle, A. Direct Spinning of CNT Fibres: Past, Present and Future Scale Up. *Carbon* **2019**, *152*, 218−232.
(19) Koziol, K.; Vilatela, J.; Moisala, A.; Motta, M.; Cunniff, P.; Sennett, M.; Windle, A. High-Performance Carbon Nanotube Fiber. *Science* **2007**, *318*, 1892−1895.
(20) Li, Y. L.; Kinloch, I. A.; Windle, A. H. Direct Spinning of Carbon Nanotube Fibers from Chemical Vapor Deposition Synthesis. *Science* **2004**, *304*, 276−278.
(21) Issman, L.; Kloza, P. A.; Terrones Portas, J.; Collins, B.; Pendashteh, A.; Pick, M.; Vilatela, J. J.; Elliott, J. A.; Boies, A. Highly Oriented Direct-Spun Carbon Nanotube Textiles Aligned by in Situ Radio-Frequency Fields. *ACS Nano* **2022**, *16*, 9583−9597.
(22) Vilatela, J. J.; Elliott, J. A.; Windle, A. H. A Model for the Strength of Yarn-Like Carbon Nanotube Fibers. *ACS Nano* **2011**, *5*, 1921−1927.
(23) Oh, E.; Cho, H.; Kim, J.; Kim, J. E.; Yi, Y.; Choi, J.; Lee, H.; Im, Y. H.; Lee, K. H.; Lee, W. J. Super-Strong Carbon Nanotube Fibers Achieved by Engineering Gas Flow and Postsynthesis Treatment. *ACS Appl. Mater. Interfaces* **2020**, *12*, 13107−13115.
(24) Bulmer, J. S.; Mizen, J. E.; Gspann, T. S.; Kaniyoor, A.; Ryley, J. B.; Kiley, P. J.; Sparkes, M. R.; O'Neill, B.; Elliott, J. A. Extreme Stretching of High G:D Ratio Carbon Nanotube Fibers Using Super-Acid. *Carbon* **2019**, *153*, 725−736.
(25) Wang, J.; Zhao, J.; Zhao, L.; Lu, Q.; Zhou, T.; Yong, Z.; Wang, P.; Zhang, X.; Li, Q. Interfacial-Bubbling-Induced Nondestructive Expansion to Reconstruct Superstrong and Multifunctional Carbon Nanotube Fibers. *Carbon* **2021**, *184*, 24−33.
(26) Zhang, Q.; Li, K.; Fan, Q.; Xia, X.; Zhang, N.; Xiao, Z.; Zhou, W.; Yang, F.; Wang, Y.; Liu, H.; Zhou, W. Performance Improvement of Continuous Carbon Nanotube Fibers by Acid Treatment. *Chin. Phys. B* **2017**, *26*, No. 028802.
(27) Lee, J.; Lee, D. M.; Jung, Y.; Park, J.; Lee, H. S.; Kim, Y. K.; Park, C. R.; Jeong, H. S.; Kim, S. M. Direct Spinning and Densification Method for High-Performance Carbon Nanotube Fibers. *Nat. Commun.* **2019**, *10*, 2962.
(28) Xu, W.; Chen, Y.; Zhan, H.; Wang, J. N. High-Strength Carbon Nanotube Film from Improving Alignment and Densification. *Nano Lett.* **2016**, *16*, 946−952.
(29) Wang, J. N.; Luo, X. G.; Wu, T.; Chen, Y. High-Strength Carbon Nanotube Fibre-Like Ribbon with High Ductility and High Electrical Conductivity. *Nat. Commun.* **2014**, *5*, 3848.
(30) Di, J.; Fang, S.; Moura, F. A.; Galvão, D. S.; Bykova, J.; Aliev, A.; de Andrade, M. J.; Lepró, X.; Li, N.; Haines, C. Strong, Twist-Stable Carbon Nanotube Yarns and Muscles by Tension Annealing at Extreme Temperatures. *Adv. Mater.* **2016**, *28*, 6598−6605.
(31) Lee, D.; Kim, S. G.; Hong, S.; Madrona, C.; Oh, Y.; Park, M.; Komatsu, N.; Taylor, L. W.; Chung, B.; Kim, J.; Strength, U. Modulus, and Conductivity of Graphitic Fibers by Macromolecular Coalescence. *Sci. Adv.* **2022**, *8*, No. eabn0939.
(32) Liu, J.; Gong, W.; Yao, Y.; Li, Q.; Jiang, J.; Wang, Y.; Zhou, G.; Qu, S.; Lu, W. Strengthening Carbon Nanotube Fibers with Semi-Crystallized Polyvinyl Alcohol and Hot-Stretching. *Compos. Sci. Technol.* **2018**, *164*, 290−295.
(33) Shi, Q. Q.; Zhan, H.; Mo, R. W.; Wang, J. N. High-Strength and Toughness Carbon Nanotube Fiber/Resin Composites by Controllable Wet-Stretching and Stepped Pressing. *Carbon* **2022**, *189*, 1−9.
(34) Li, S.; Zhang, X.; Zhao, J.; Meng, F.; Xu, G.; Yong, Z.; Jia, J.; Zhang, Z.; Li, Q. Enhancement of Carbon Nanotube Fibres Using Different Solvents and Polymers. *Compos. Sci. Technol.* **2012**, *72*, 1402−1407.
(35) Yin, Z.; Liang, X.; Zhou, K.; Li, S.; Lu, H.; Zhang, M.; Wang, H.; Xu, Z.; Zhang, Y. Biomimetic Mechanically Enhanced Carbon Nanotube Fibers by Silk Fibroin Infiltration. *Small* **2021**, *17*, No. 2100066.
(36) Park, O. K.; Choi, H.; Jeong, H.; Jung, Y.; Yu, J.; Lee, J. K.; Hwang, J. Y.; Kim, S. M.; Jeong, Y.; Park, C. R.; Endo, M.; Ku, B. C. High-Modulus and Strength Carbon Nanotube Fibers Using Molecular Cross-Linking. *Carbon* **2017**, *118*, 413−421.
(37) Lepak-Kuc, S.; Milowska, K. Z.; Boncel, S.; Szybowicz, M.; Dychalska, A.; Jozwik, I.; Koziol, K. K.; Jakubowska, M.; Lekawa-Raus, A. Highly Conductive Doped Hybrid Carbon Nanotube-Graphene Wires. *ACS Appl. Mater. Interfaces* **2019**, *11*, 33207−33220.
(38) Wang, Y.; Colas, G.; Filleter, T. Improvements in the Mechanical Properties of Carbon Nanotube Fibers through Graphene Oxide Interlocking. *Carbon* **2016**, *98*, 291−299.
(39) Kim, Y. J.; Park, J.; Yang, C. M.; Jeong, H. S.; Kim, S. M.; Han, S. W.; Yang, B.; Kim, Y. K. Bio-Inspired Incorporation of Functionalized Graphene Oxide into Carbon Nanotube Fibers for Their Efficient Mechanical Reinforcement. *Compos. Sci. Technol.* **2019**, *181*, No. 107680.
(40) Nam, K. H.; Im, Y. O.; Park, H. J.; Lee, H.; Park, J.; Jeong, S.; Kim, S. M.; You, N. H.; Choi, J. H.; Han, H.; Lee, K. H.; Ku, B. C. Photoacoustic Effect on the Electrical and Mechanical Properties of Polymer-Infiltrated Carbon Nanotube Fiber/Graphene Oxide Composites. *Compos. Sci. Technol.* **2017**, *153*, 136−144.
(41) Chang, S.; Lou, H.; Meng, W.; Li, M.; Guo, F.; Pang, R.; Xu, J.; Zhang, Y.; Shang, Y.; Cao, A. Carbon Nanotube/Polymer Coaxial Cables with Strong Interface for Damping Composites and Stretchable Conductors. *Adv. Funct. Mater.* **2022**, *32*, No. 2112231.
(42) Gong, Q.; Yu, Y.; Kang, L.; Zhang, M.; Zhang, Y.; Wang, S.; Niu, Y.; Zhang, Y.; Di, J.; Li, Q.; Zhang, J. Modulus-Tailorable, Stretchable, and Biocompatible Carbonene Fiber for Adaptive Neural Electrode. *Adv. Funct. Mater.* **2021**, *32*, No. 2107360.
(43) Ryu, S.; Chou, J. B.; Lee, K.; Lee, D.; Hong, S. H.; Zhao, R.; Lee, H.; Kim, S. G. Direct Insulation-to-Conduction Transformation of Adhesive Catecholamine for Simultaneous Increases of Electrical Conductivity and Mechanical Strength of CNT Fibers. *Adv. Mater.* **2015**, *27*, 3250−3255.
(44) Li, M.; Song, Y.; Zhang, C.; Yong, Z.; Qiao, J.; Hu, D.; Zhang, Z.; Wei, H.; Di, J.; Li, Q. Robust Carbon Nanotube Composite Fibers: Strong Resistivities to Protonation, Oxidation, and Ultrasonication. *Carbon* **2019**, *146*, 627−635.
(45) Zhang, S.; Hao, A.; Nguyen, N.; Oluwalowo, A.; Liu, Z.; Dessureault, Y.; Park, J. G.; Liang, R. Carbon Nanotube/Carbon Composite Fiber with Improved Strength and Electrical Conductivity Via Interface Engineering. *Carbon* **2019**, *144*, 628−638.
(46) Ramesh, S.; Ericson, L. M.; Davis, V. A.; Saini, R. K.; Kittrell, C.; Pasquali, M.; Billups, W.; Adams, W. W.; Hauge, R. H.; Smalley, R. E. Dissolution of Pristine Single Walled Carbon Nanotubes in Superacids by Direct Protonation. *J. Phys. Chem. B* **2004**, *108*, 8794−8798.

https://doi.org/10.1021/acsami.2c21518
ACS Appl. Mater. Interfaces 2023, 15, 5701−5708

(47) Ericson, L. M.; Fan, H.; Peng, H.; Davis, V. A.; Zhou, W.; Sulpizio, J.; Wang, Y.; Booker, R.; Vavro, J.; Guthy, C.; Parra-Vasquez, A. N. G.; Kim, M. J.; Ramesh, S.; Saini, R. K.; Kittrell, C.; Lavin, G.; Schmidt, H.; Adams, W. W.; Billups, W. E.; Pasquali, M.; Hwang, W. F.; Hauge, R. H.; Fischer, J. E.; Smalley, R. E. Macroscopic, Neat, Single-Walled Carbon Nanotube Fibers. *Science* **2004**, *305*, 1447−1450.
(48) Zhou, W.; Heiney, P. A.; Fan, H.; Smalley, R. E.; Fischer, J. E. Single-Walled Carbon Nanotube-Templated Crystallization of H_2SO_4: Direct Evidence for Protonation. *J. Am. Chem. Soc.* **2005**, *127*, 1640−1641.
(49) Sun, Y.; Chen, Z.; Gong, H.; Li, X.; Gao, Z.; Xu, S.; Han, X.; Han, B.; Meng, X.; Zhang, J. Continuous ″Snowing″ Thermotherapeutic Graphene. *Adv. Mater.* **2020**, *32*, No. 2002024.
(50) Sun, Y.; Yang, L.; Xia, K.; Liu, H.; Han, D.; Zhang, Y.; Zhang, J. ″Snowing″ Graphene Using Microwave Ovens. *Adv. Mater.* **2018**, *30*, No. 1803189.
(51) Behabtu, N.; Lomeda, J. R.; Green, M. J.; Higginbotham, A. L.; Sinitskii, A.; Kosynkin, D. V.; Tsentalovich, D.; Parra-Vasquez, A. N.; Schmidt, J.; Kesselman, E.; Cohen, Y.; Talmon, Y.; Tour, J. M.; Pasquali, M. Spontaneous High-Concentration Dispersions and Liquid Crystals of Graphene. *Nat. Nanotechnol.* **2010**, *5*, 406−411.
(52) Brandley, E.; Greenhalgh, E. S.; Shaffer, M. S. P.; Li, Q. Mapping Carbon Nanotube Orientation by Fast Fourier Transform of Scanning Electron Micrographs. *Carbon* **2018**, *137*, 78−87.
(53) Kaniyoor, A.; Gspann, T. S.; Mizen, J. E.; Elliott, J. A. Quantifying Alignment in Carbon Nanotube Yarns and Similar Two-Dimensional Anisotropic Systems. *J. Appl. Polym. Sci.* **2021**, *138*, 50939.
(54) Wan, S.; Chen, Y.; Fang, S.; Wang, S.; Xu, Z.; Jiang, L.; Baughman, R. H.; Cheng, Q. High-Strength Scalable Graphene Sheets by Freezing Stretch-Induced Alignment. *Nat. Mater.* **2021**, *20*, 624−631.
(55) Zhang, F.; Ren, D.; Huang, L.; Zhang, Y.; Sun, Y.; Liu, D.; Zhang, Q.; Feng, W.; Zheng, Q. 3D Interconnected Conductive Graphite Nanoplatelet Welded Carbon Nanotube Networks for Stretchable Conductors. *Adv. Funct. Mater.* **2021**, *31*, No. 2107082.
(56) Foroughi, J.; Spinks, G. M.; Antiohos, D.; Mirabedini, A.; Gambhir, S.; Wallace, G. G.; Ghorbani, S. R.; Peleckis, G.; Kozlov, M. E.; Lima, M. D.; Baughman, R. H. Highly Conductive Carbon Nanotube-Graphene Hybrid Yarn. *Adv. Funct. Mater.* **2014**, *24*, 5859−5865.
(57) Liu, P.; Li, Y.; Xu, Y.; Bao, L.; Wang, L.; Pan, J.; Zhang, Z.; Sun, X.; Peng, H. Stretchable and Energy-Efficient Heating Carbon Nanotube Fiber by Designing a Hierarchically Helical Structure. *Small* **2018**, *14*, No. 1702926.
(58) Wang, R.; Xu, Z.; Zhuang, J.; Liu, Z.; Peng, L.; Li, Z.; Liu, Y.; Gao, W.; Gao, C. Highly Stretchable Graphene Fibers with Ultrafast Electrothermal Response for Low-Voltage Wearable Heaters. *Adv. Electron. Mater.* **2017**, *3*, No. 1600425.
(59) Hong, S.; Lee, H.; Lee, J.; Kwon, J.; Han, S.; Suh, Y. D.; Cho, H.; Shin, J.; Yeo, J.; Ko, S. H. Highly Stretchable and Transparent Metal Nanowire Heater for Wearable Electronics Applications. *Adv. Mater.* **2015**, *27*, 4744−4751.
(60) Ji, S.; He, W.; Wang, K.; Ran, Y.; Ye, C. Thermal Response of Transparent Silver Nanowire/PEDOT: PSS Film Heaters. *Small* **2014**, *10*, 4951−4960.
(61) Liu, P.; Liu, L.; Jiang, K.; Fan, S. Carbon-Nanotube-Film Microheater on a Polyethylene Terephthalate Substrate and Its Application in Thermochromic Displays. *Small* **2011**, *7*, 732−736.
(62) Sui, D.; Huang, Y.; Huang, L.; Liang, J.; Ma, Y.; Chen, Y. Flexible and Transparent Electrothermal Film Heaters Based on Graphene Materials. *Small* **2011**, *7*, 3186−3192.
(63) Liu, P.; Fan, Z.; Mikhalchan, A.; Tran, T. Q.; Jewell, D.; Duong, H. M.; Marconnet, A. M. Continuous Carbon Nanotube-Based Fibers and Films for Applications Requiring Enhanced Dissipation. *ACS Appl. Mater. Interfaces* **2016**, *8*, 17461−17471.
(64) Liu, P.; Liu, L.; Wei, Y.; Liu, K.; Chen, Z.; Jiang, K.; Li, Q.; Fan, S. Fast High-Temperature Response of Carbon Nanotube Film and Its Application as an Incandescent Display. *Adv. Mater.* **2009**, *21*, 3563−3566.
(65) Yuan, H.; Zhang, H.; Huang, K.; Cheng, Y.; Wang, K.; Cheng, S.; Li, W.; Jiang, J.; Li, J.; Tu, C.; Wang, X.; Qi, Y.; Liu, Z. Dual-Emitter Graphene Glass Fiber Fabric for Radiant Heating. *ACS Nano* **2022**, *16*, 2577−2584.
(66) Sun, J.; Wang, Y.; Liao, W.; Yang, Z. Ultrafast, High-Contractile Electrothermal-Driven Liquid Crystal Elastomer Fibers Towards Artificial Muscles. *Small* **2021**, *17*, No. 2103700.
(67) Niu, Y.; Zhou, T.; Li, Z.; Wang, B.; Dong, S.; Zhou, S.; Wu, K.; Yong, Z.; Zhang, Y. High-Strength Carbon Nanotube Fibers with near 100% Purity Acquired Via Isothermal Vacuum Annealing. *Diamond Relat. Mater.* **2021**, *116*, No. 108391.
(68) Zhou, T.; Niu, Y.; Li, Z.; Li, H.; Yong, Z.; Wu, K.; Zhang, Y.; Li, Q. The Synergetic Relationship between the Length and Orientation of Carbon Nanotubes in Direct Spinning of High-Strength Carbon Nanotube Fibers. *Mater. Design* **2021**, *203*, No. 109557.

https://doi.org/10.1021/acsami.2c21518
ACS Appl. Mater. Interfaces 2023, 15, 5701−5708